Supplementary Figure 1

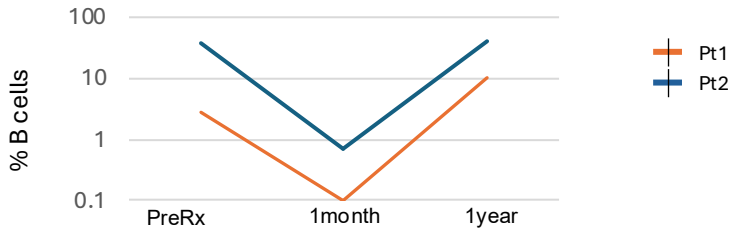

Supplementary Figure 1| Kinetics of B cell reconstitution following rituximab treatment

Representative longitudinal profiles showing B cell depletion and subsequent recovery following a single cycle of rituximab in 2 different patients on ARM-B.

Supplementary Figure 2

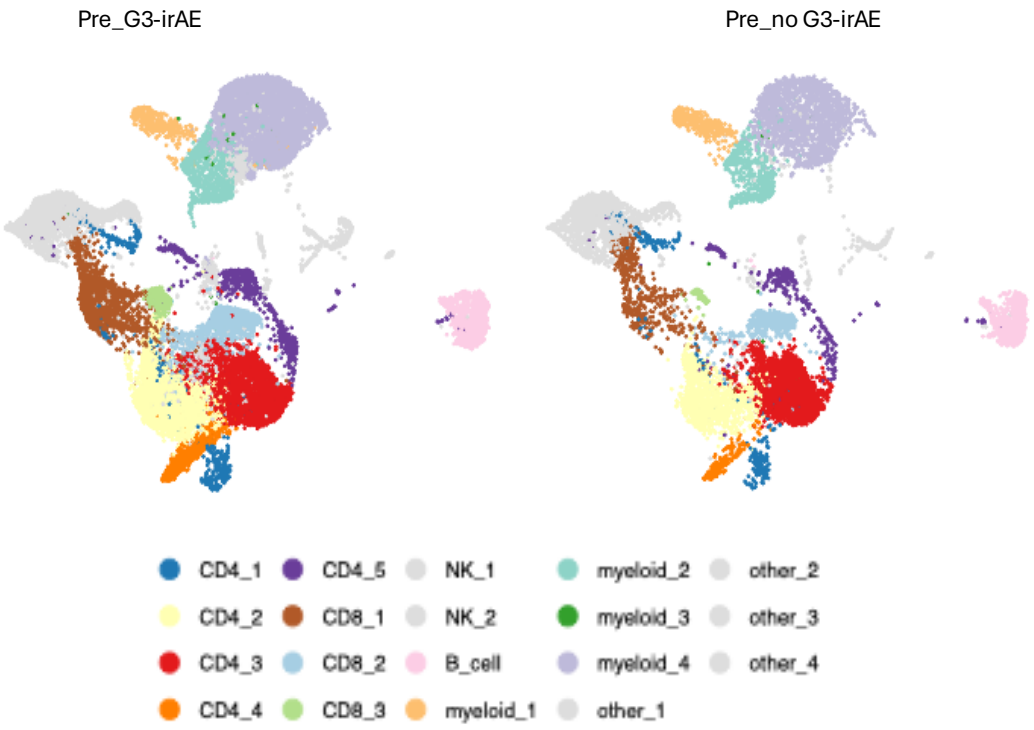

Supplementary Figure 2 | Cellular clusters and interaction networks used for CellChat analysis at pretreatment in Arm-A

UMAP representation of pretreatment Arm-A samples showing the annotated cellular clusters used as input for CellChat analysis.

Supplementary Figure 3

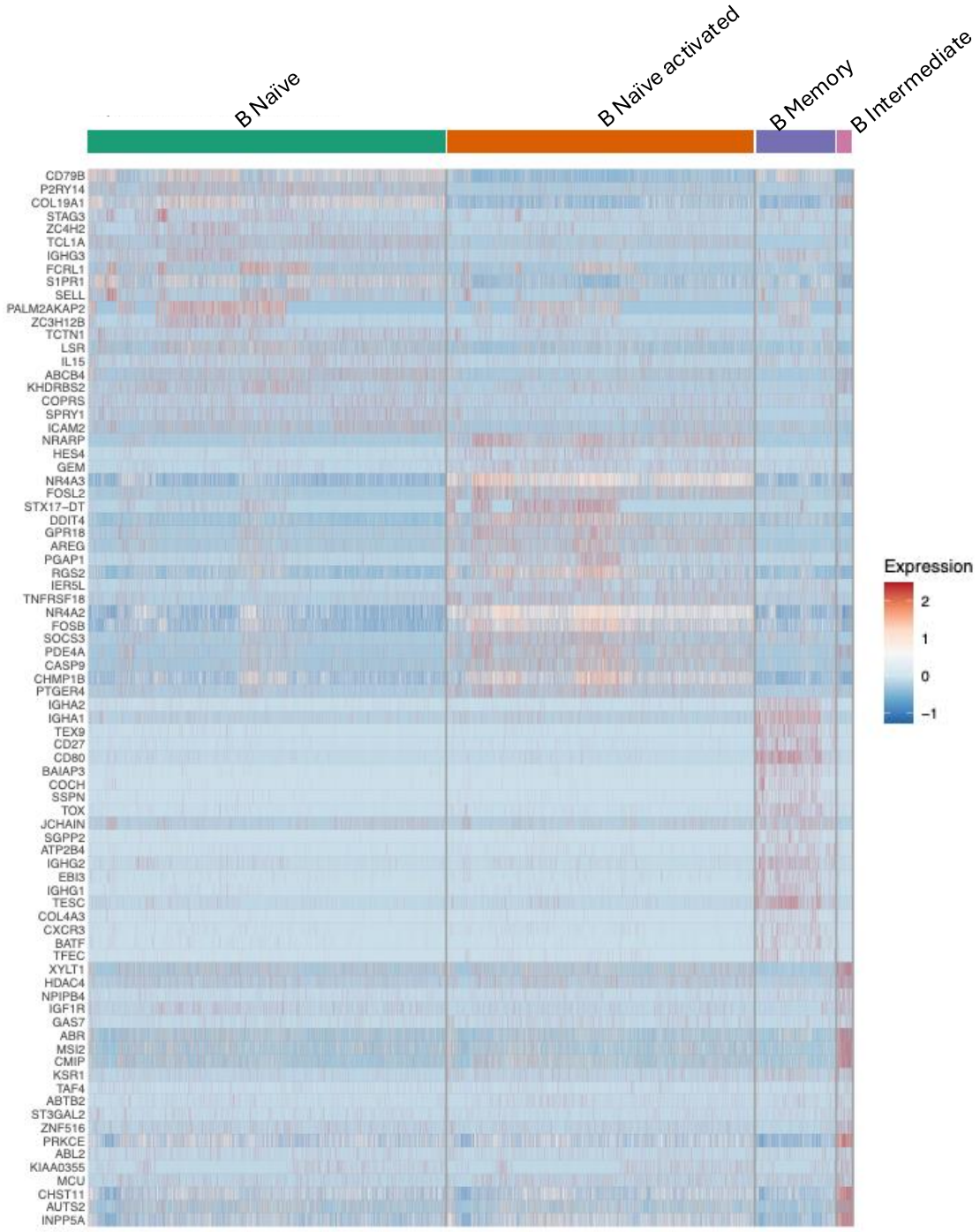

Supplementary Figure 3 | Differential gene expression across B cell clusters
Heatmap summarizing differentially expressed genes across transcriptionally defined B cell clusters.

Supplementary Figure 4

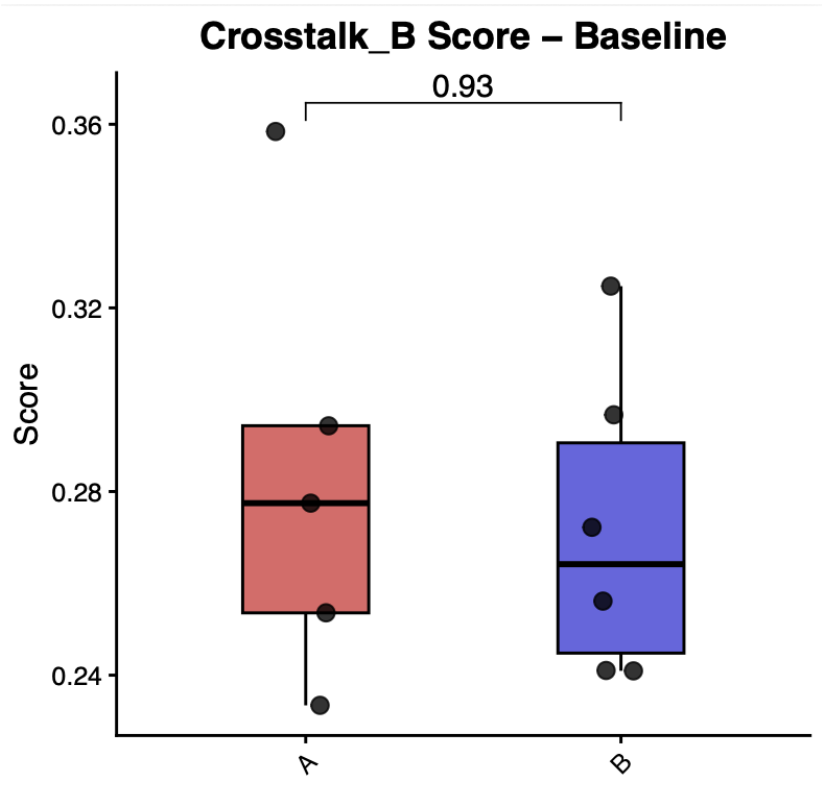

Supplementary Figure 4. Comparison of B cell crosstalk scores between treatment arms. Pseudobulk analysis of the signature_1autoB score in B cells at baseline, stratified by treatment arm A (red) and arm B (blue). Each data point represents the mean expression score calculated per individual sample. Statistical significance was evaluated using a two-sided Wilcoxon rank-sum test.

Supplementary Figure 5

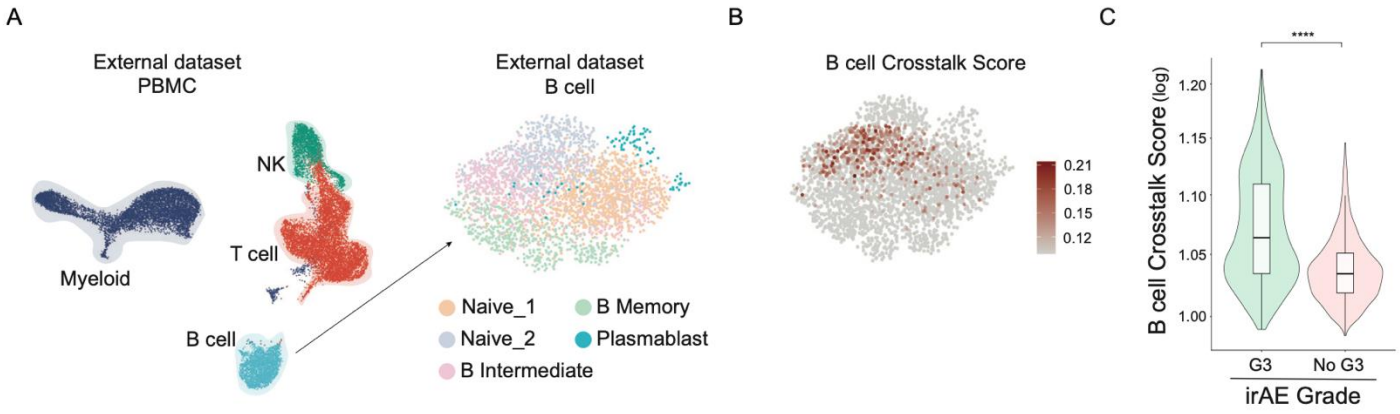

Supplementary Figure 5. B cell crosstalk signature in an independent cohort. Publicly available single-cell RNA-sequencing data from Lozano et al. (Nat Med 2022) were analyzed. PBMCs from patients who received combination checkpoint blockade therapy were integrated (n = 14; 22,462 cells).
(A) UMAP embedding of integrated PBMCs showing main immune cell compartments, including T cells, NK cells, myeloid cells, and B cells (left). UMAP embedding of re-clustered B cells (n = 2,963 cells) displaying main B cell cluster identities (right).
(B) Feature plot highlighting B cells with B cell crosstalk scores in the 80th percentile (dark red).
(**C**) Violin plot showing the distribution of the B cell crosstalk score stratified by irAE severity (G3-irAE vs. no G3-irAE).
Box plots within the violins represent the median and interquartile range in C.
****P <0.0001. Two-tailed Wilcoxon rank-sum test was used for statistical analysis in C. Statistical analyses for differential expression between main cell compartments were performed using the Wilcoxon rank-sum test with Benjamini-Hochberg correction.

Supplementary Figure 6

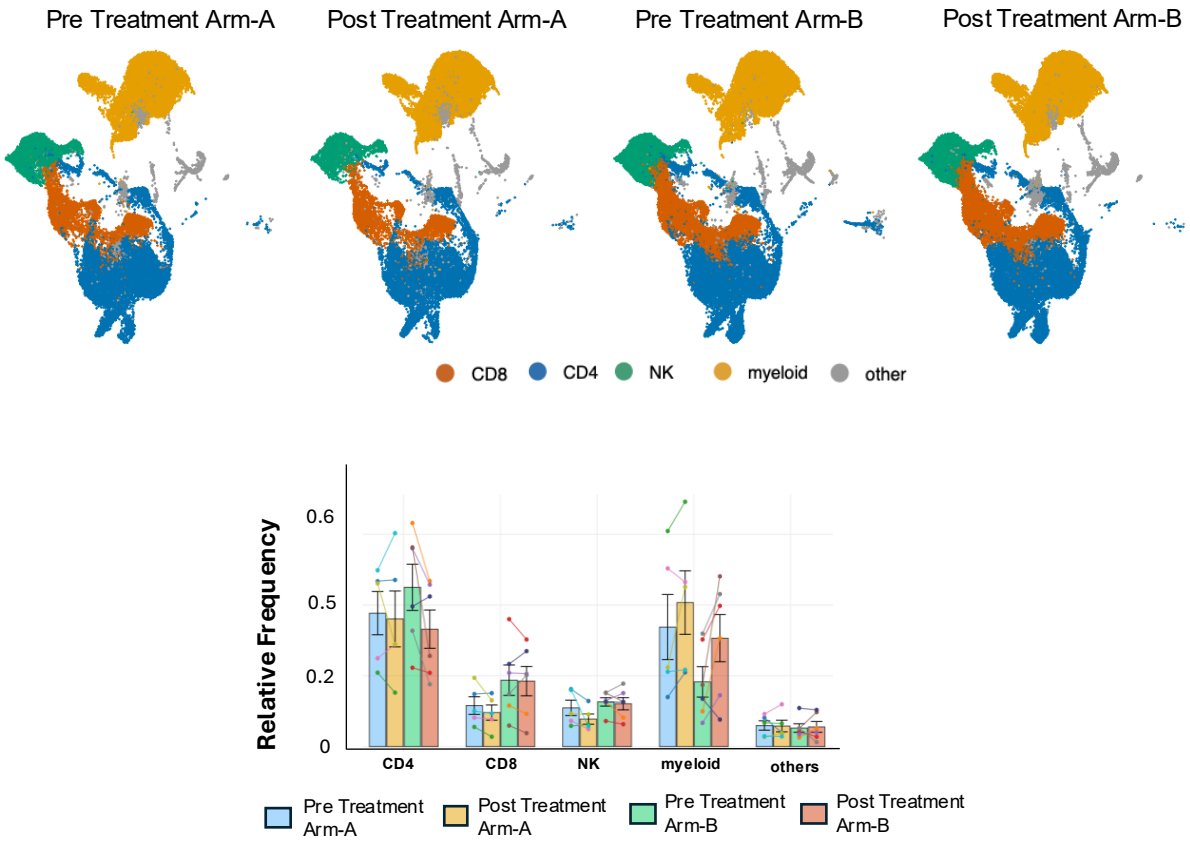

Supplementary Figure 6 | Single-cell transcriptomic cluster frequencies after exclusion of B cells

Relative frequencies of scRNA-seq–defined cellular clusters after exclusion of B cells from the analysis. UMAP embeddings (top panel) and corresponding cell proportions (bottom graph).

Supplementary Figure 7

A CD4 Metacluster proportions by arm and timepoint

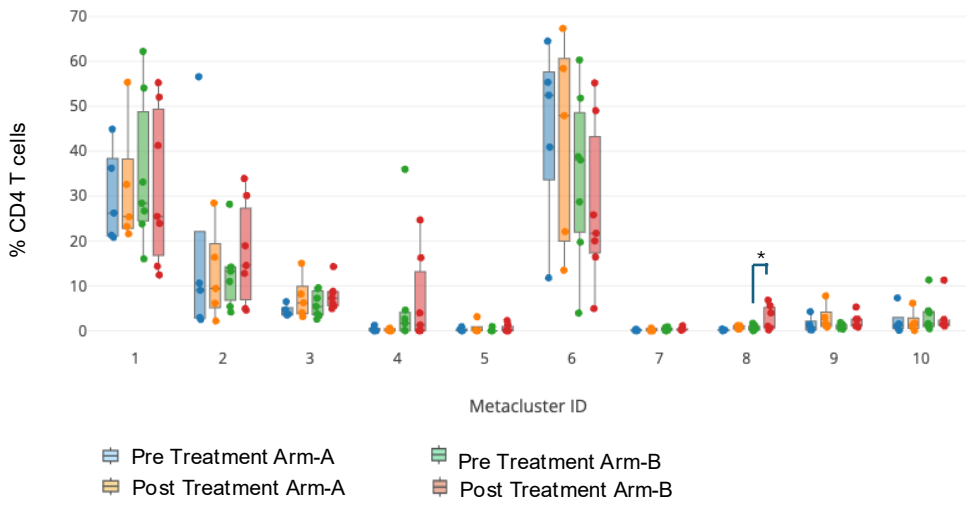

B CD8 Metacluster proportions by arm and timepoint

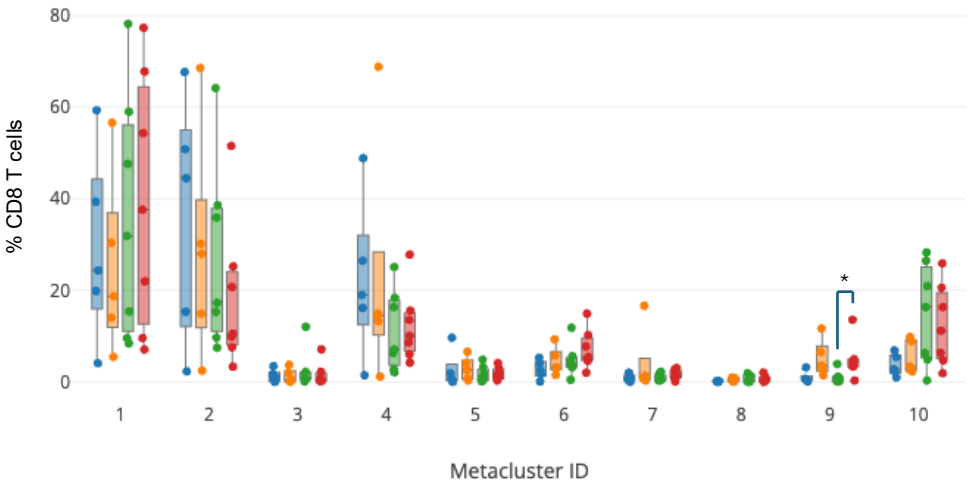

Supplementary Figure 7 | Distribution of T cells in metaclusters identified by single cell mass cytometry.
(A) CD4+ T cell proportions across 10 CD4 metaclusters.
(B) CD8+ T cell proportions across 10 CD8 metaclusters.

Supplementary Figure 8

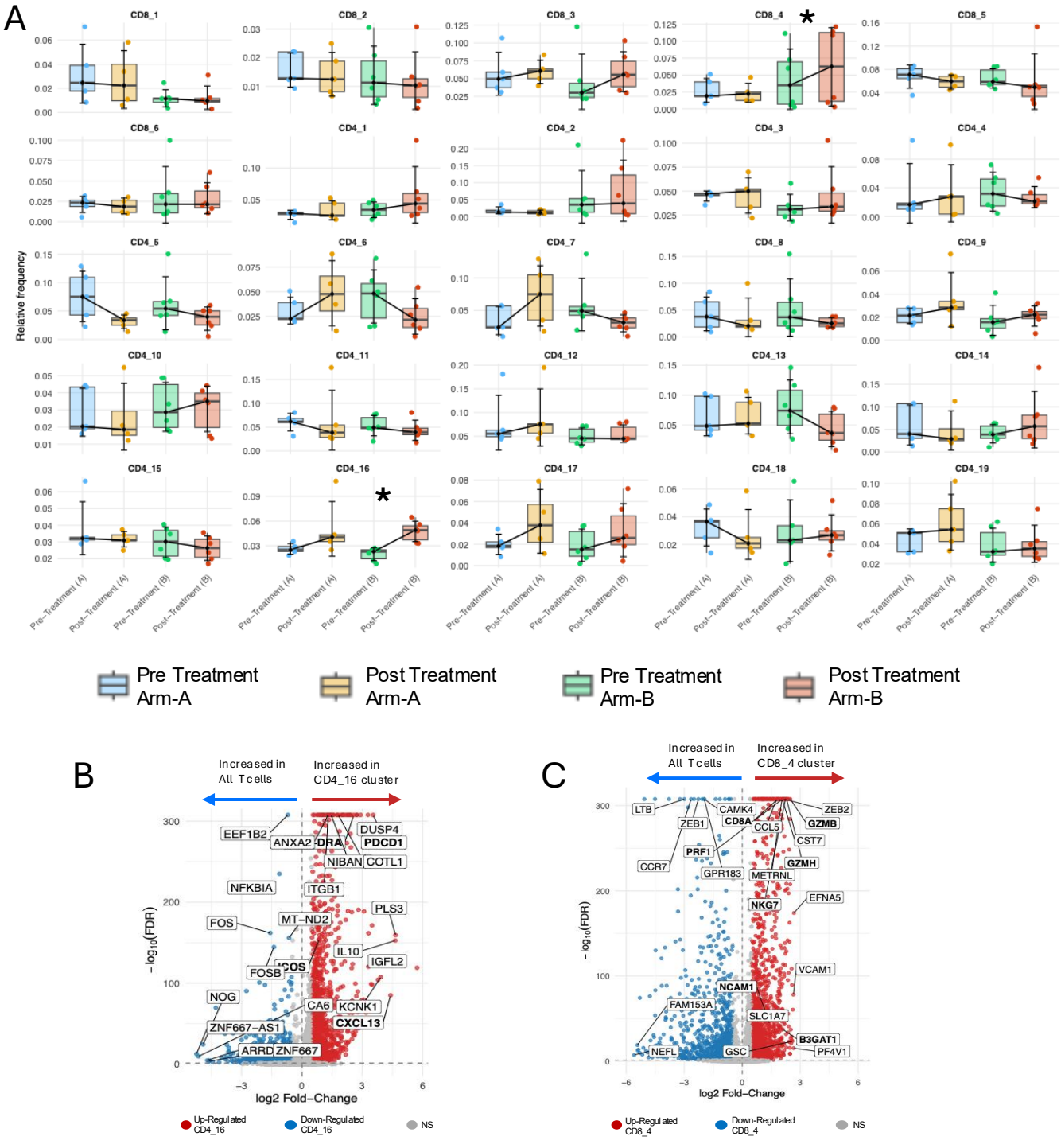

Supplementary Figure 8 | Transcriptional and compositional changes in T cell compartments

(A) Boxplots showing relative frequencies of T cell clusters in Arm-A and Arm-B, comparing pretreatment and post-treatment samples.

(B) Volcano plot depicting differentially expressed genes in the CD4_16 cluster compared with all other T cells.

(C) Volcano plot depicting differentially expressed genes in the CD8_4 cluster compared with all other T cells.

Supplementary Figure 9

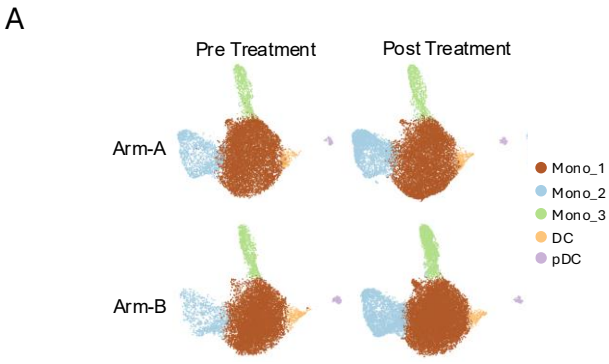

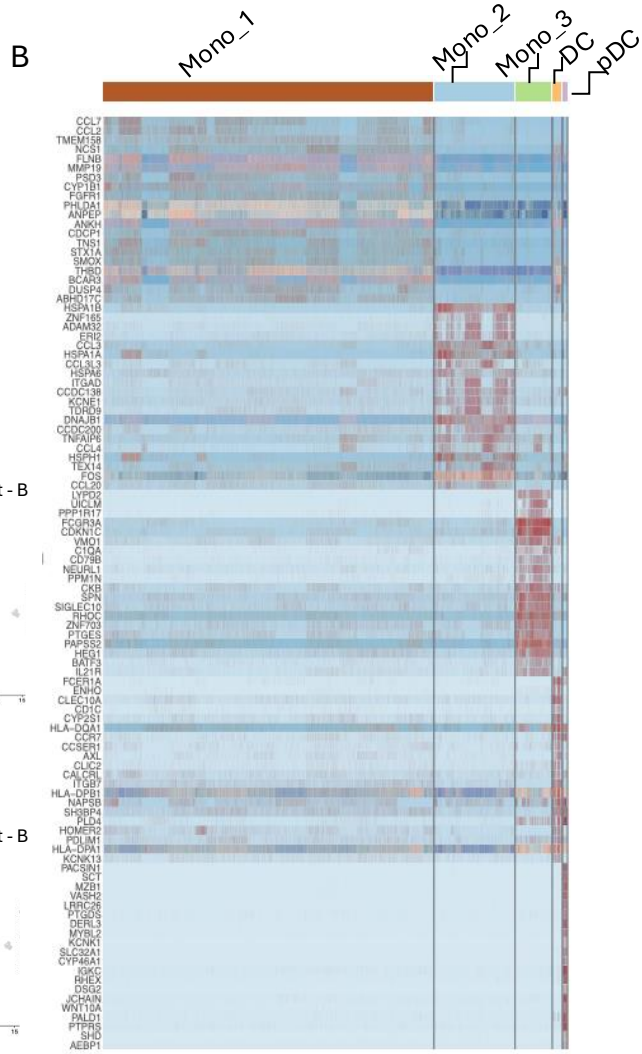

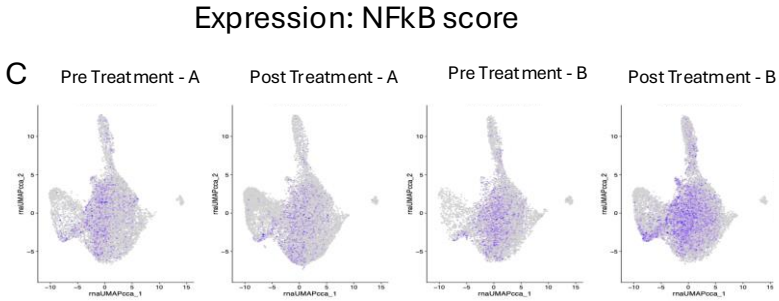

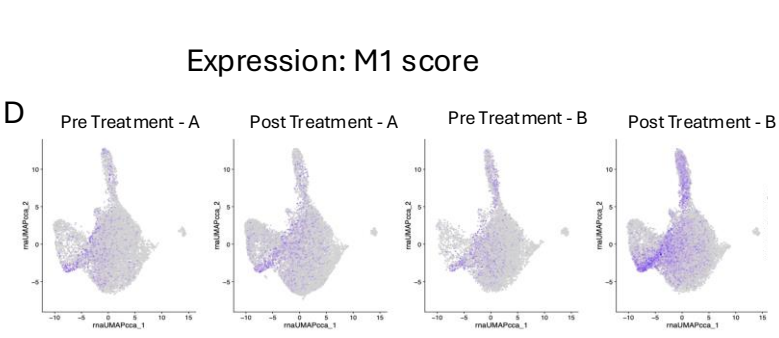

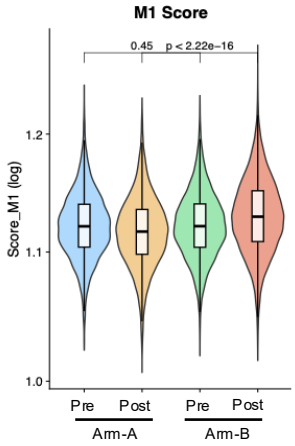

Supplementary Figure 9 | Remodeling of myeloid cell populations following treatment

(A) UMAP visualization of transcriptionally defined myeloid cell clusters.

(B) Heatmap showing differentially expressed genes across myeloid clusters.

(C) Feature plot of myeloid cells highlighting cells within the 80th percentile of the NF-κB signature score.

(D) Feature plot (top) showing myeloid cells within the 80th percentile of the M1 polarization score, with corresponding violin plots (bottom) summarizing M1 scores across myeloid populations.

Supplementary Figure 10

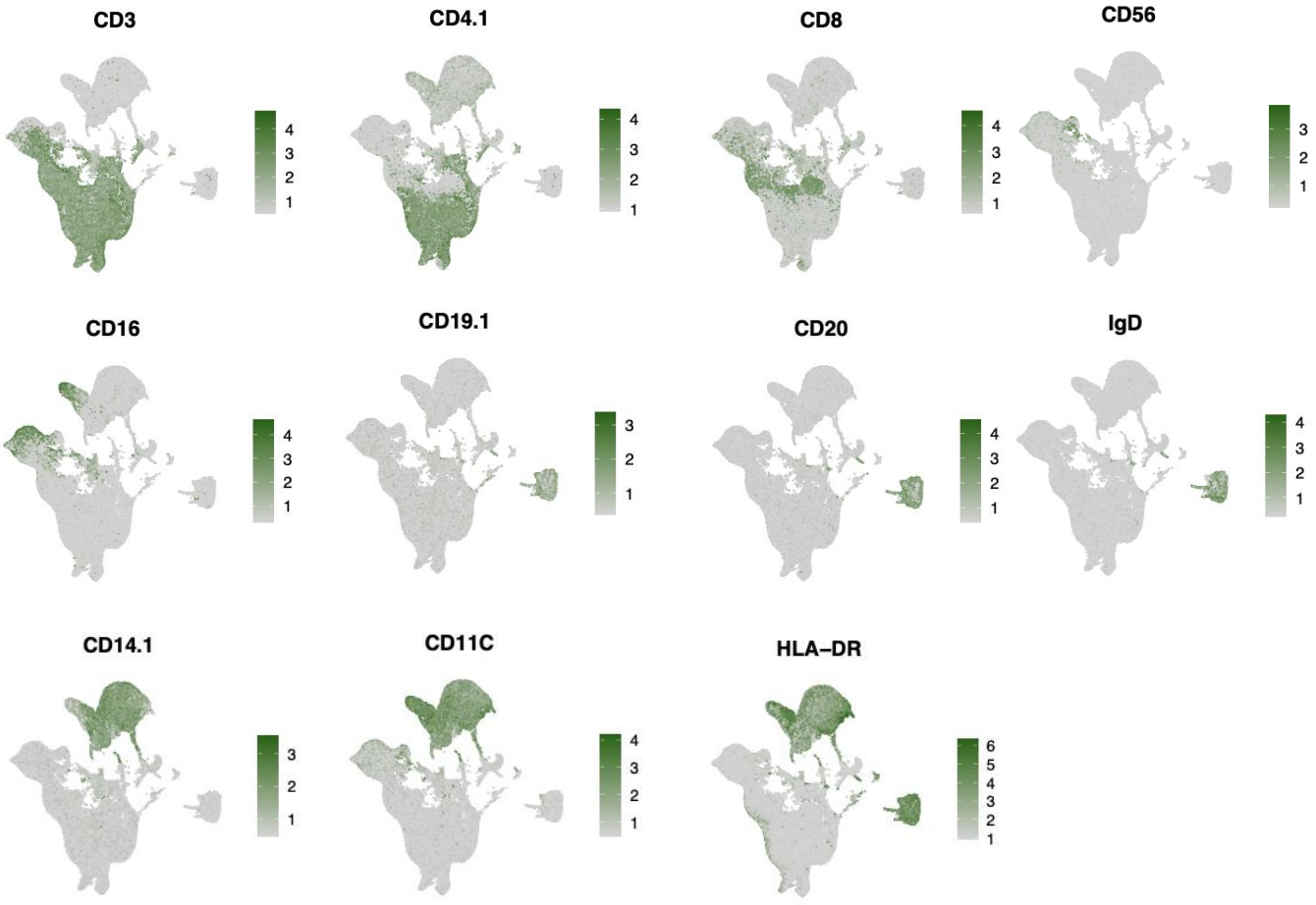

Supplementary Figure 10 | ADT expression profile
Feature plots showing ADT expression profile of main cell-type markers